

Subcell Modelling of the Digital Human Phantom (DHP) in the Finite-Difference Time-Domain (FDTD) Method

Kenan Tekbas, Fumie Costen, Jean-Pierre Bérenger

The University of Manchester

kenan.tekbas@manchester.ac.uk

Basics of the FDTD Method

- The standard FDTD method [1] solves space and time derivatives of Maxwell's curl equations in the time domain using the central difference approximations.
- The method is powerful and robust for solving electromagnetic problems in broadband simulations; it provides a solution for a large number of scattering and interaction electromagnetic problems for wide range of frequencies in a single simulation run.
- However, the uniform rectangular grid structure of the FDTD method demands excessively high computational resources to resolve electrically-fine geometrical features in the problem space.

Subcell Technique

- The standard FDTD method, the entire problem space must be sampled at a scale equal to or smaller than the thickness of the layer. This spatial constraint typically causes very fine meshing of the entire problem space of interest.
- The fine spatial sampling results in excessively large memory consumption due to a dramatic increase of the total number of cells. The small size usage leads to a small time step under stability the condition, therefore an unreasonable computational time is required even for a simple engineering problem containing an electrically-fine geometrical features.

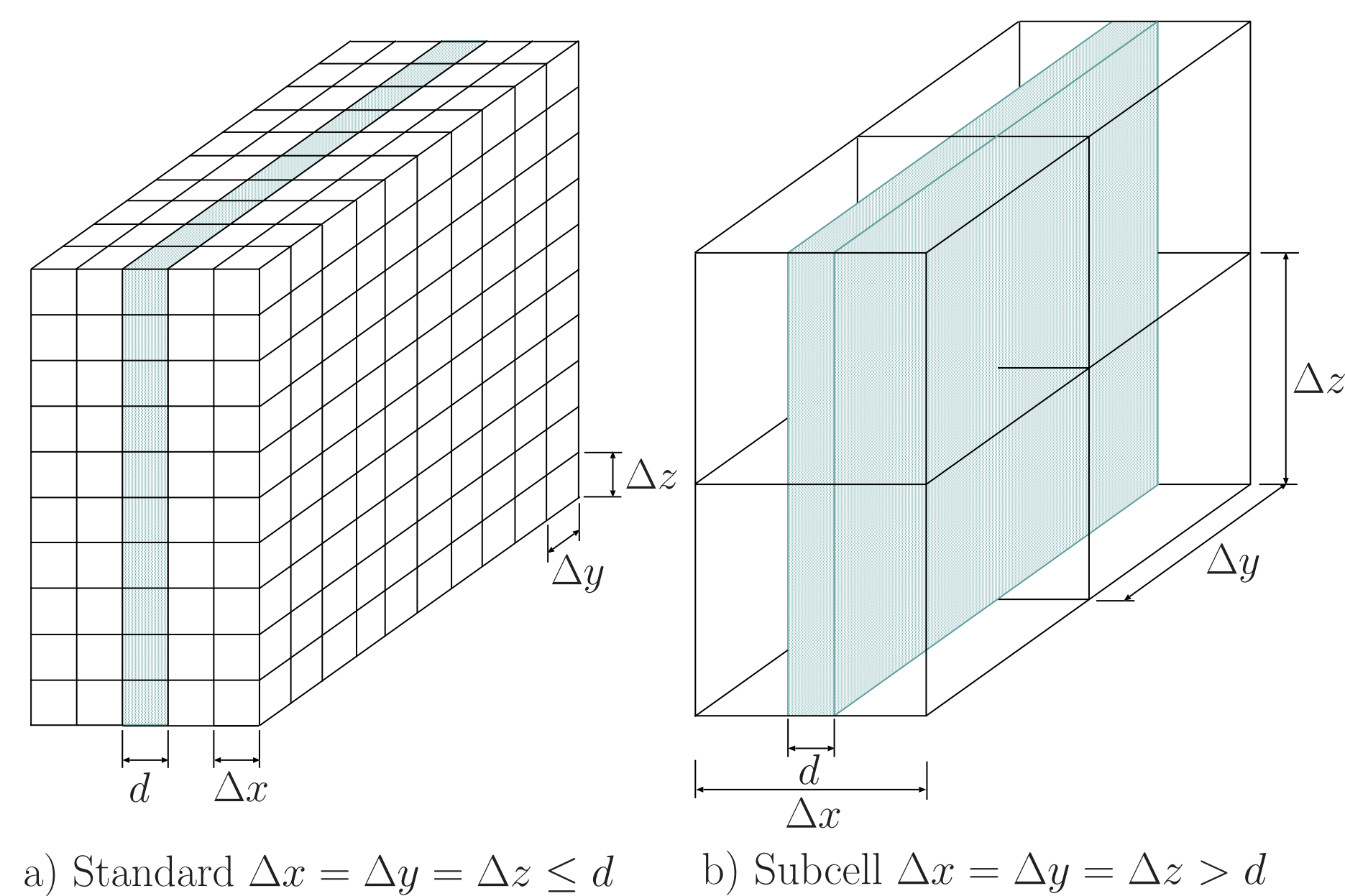


Figure 1: Meshing of the problem space.

- The subcell model permits the user to choose an FDTD cell size greater than the object thickness .
- The model relies on the application of the integral form of Ampere's law to the cell that contains the thin layer [2] .

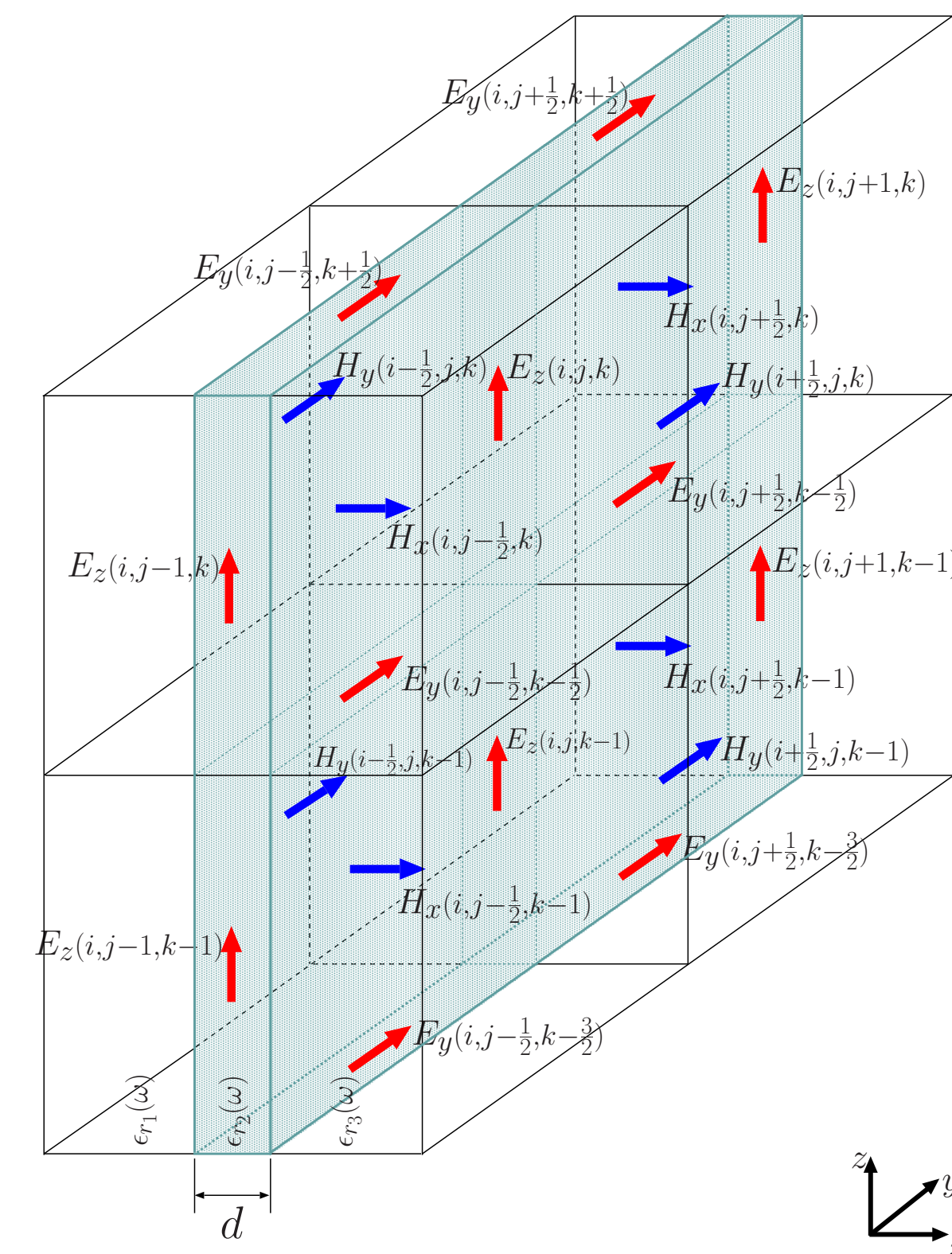


Figure 2: Thin layer and the electric and magnetic field components in the three-dimensional grid.

The Digital Human Phantom (DHP)

- To test human body's response to electromagnetic radiation without exposing a human volunteer at any risk.
- To perform any number of tests at far lower cost than actual clinical trials.

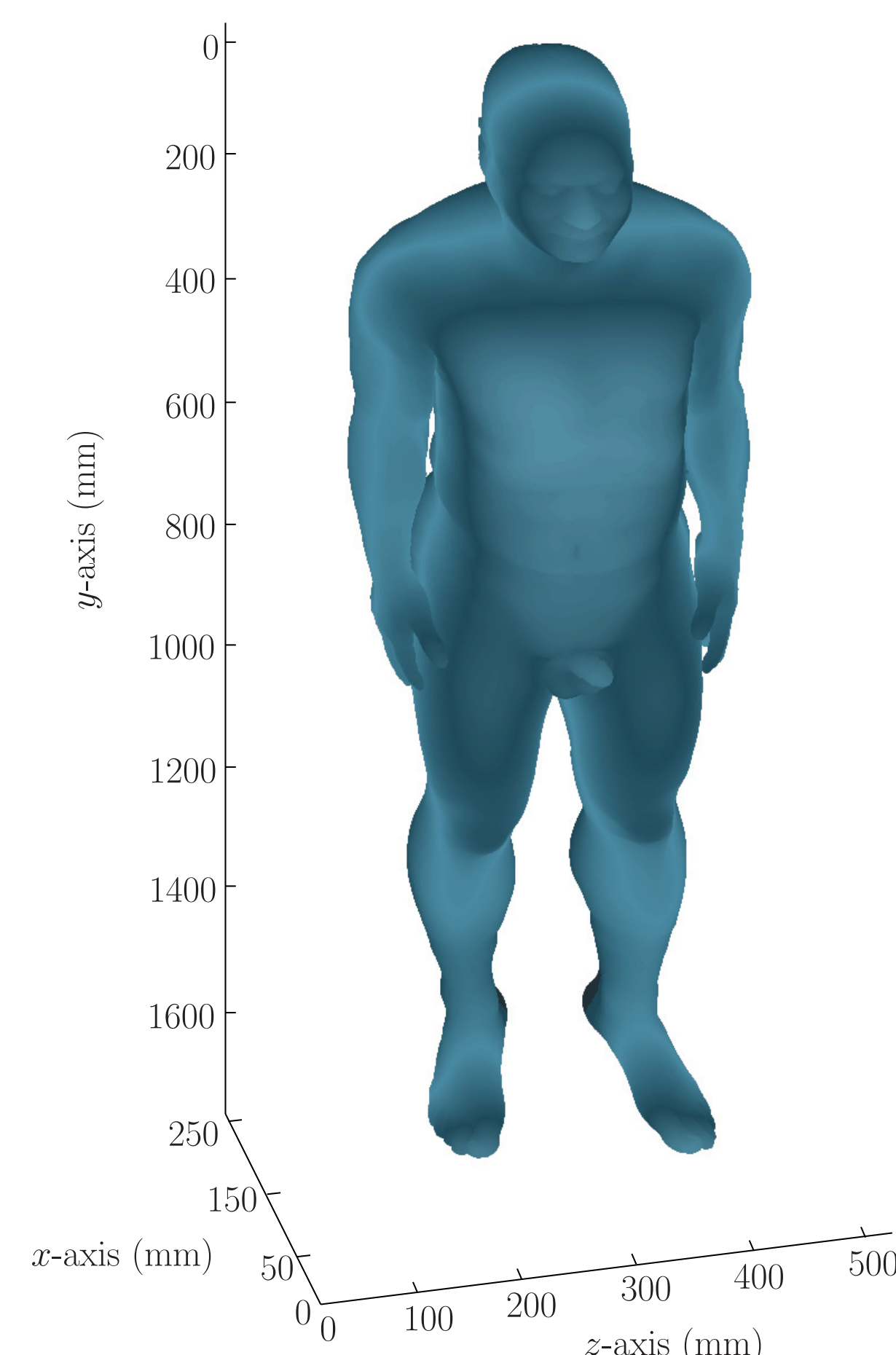


Figure 3: Three-dimensional Digital Human Phantom (DHP) created by combining 1654 cross-sectional MRI scans, taken at 1 mm intervals from the head to feet, of the healthy subject.

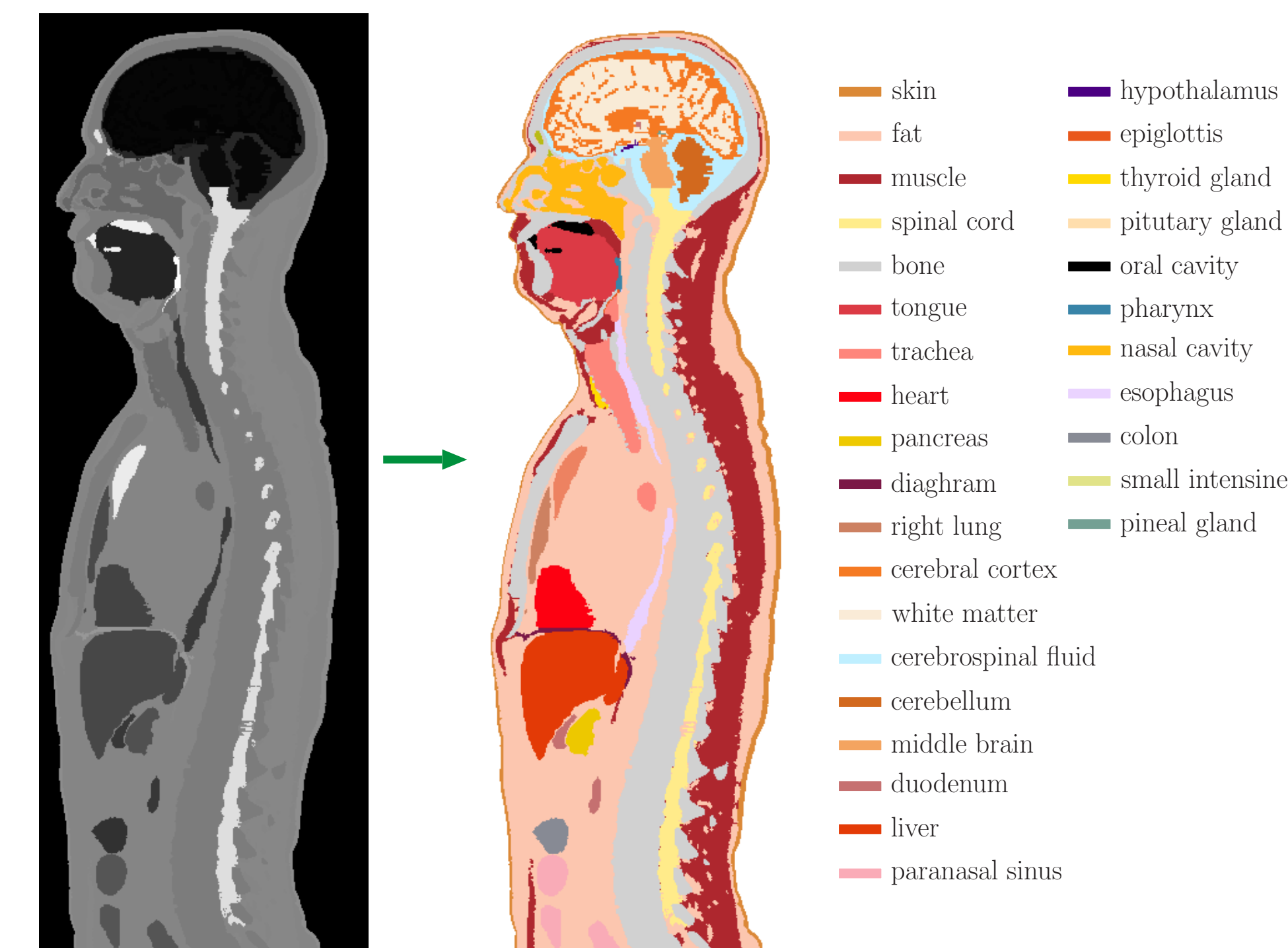


Figure 4: A slice of the digital human phantom showing the location of the tissues

- We used the Debye model to describe the electrical properties of the human tissues

$$\epsilon_r(\omega) = \epsilon_\infty + \frac{\epsilon_S - \epsilon_\infty}{1 + j\omega\tau} + \frac{\sigma_S}{j\omega\epsilon_0}$$

- Each tissue is identified with a unique ID number - 49 (Muscle), 48 (Fat) - and calls its own parameters, ϵ_∞ , ϵ_S , τ and σ_S to solve the subcell equation in each coarse cell

$$E_z^{n+1} = \gamma_1 \left[\Psi_z^{n+1} + \gamma_2 E_z^n - \gamma_3 E_z^{n-1} - \sum_{m=1}^M (s_m \zeta_{1m} D_m^n - s_m \zeta_{2m} D_m^{n-1}) \right]$$

$$\text{where } \gamma_1 = \left(\sum_{m=1}^M \xi_{1m} s_m \right)^{-1}, \quad \gamma_2 = \sum_{m=1}^M \xi_{2m} s_m, \quad \gamma_3 = \sum_{m=1}^M \xi_{3m} s_m$$

$$\text{and } \xi_{1m} = \frac{2\epsilon_0\epsilon_\infty\tau_m + 2(\epsilon_0\epsilon_{S_m} + \sigma_{S_m}\tau_m)\Delta t + \sigma_{S_m}(\Delta t)^2}{2(\Delta t + \tau_m)},$$

$$\xi_{2m} = \frac{4\epsilon_0\epsilon_\infty\tau_m + 2(\epsilon_0\epsilon_{S_m} + \sigma_{S_m}\tau_m)\Delta t - \sigma_{S_m}(\Delta t)^2}{2(\Delta t + \tau_m)},$$

$$\xi_{3m} = \frac{\epsilon_0\epsilon_\infty\tau_m}{\Delta t + \tau_m}, \quad \zeta_{1m} = \frac{\Delta t + 2\tau_m}{\Delta t + \tau_m}, \quad \zeta_{2m} = \frac{\tau_m}{\Delta t + \tau_m}.$$

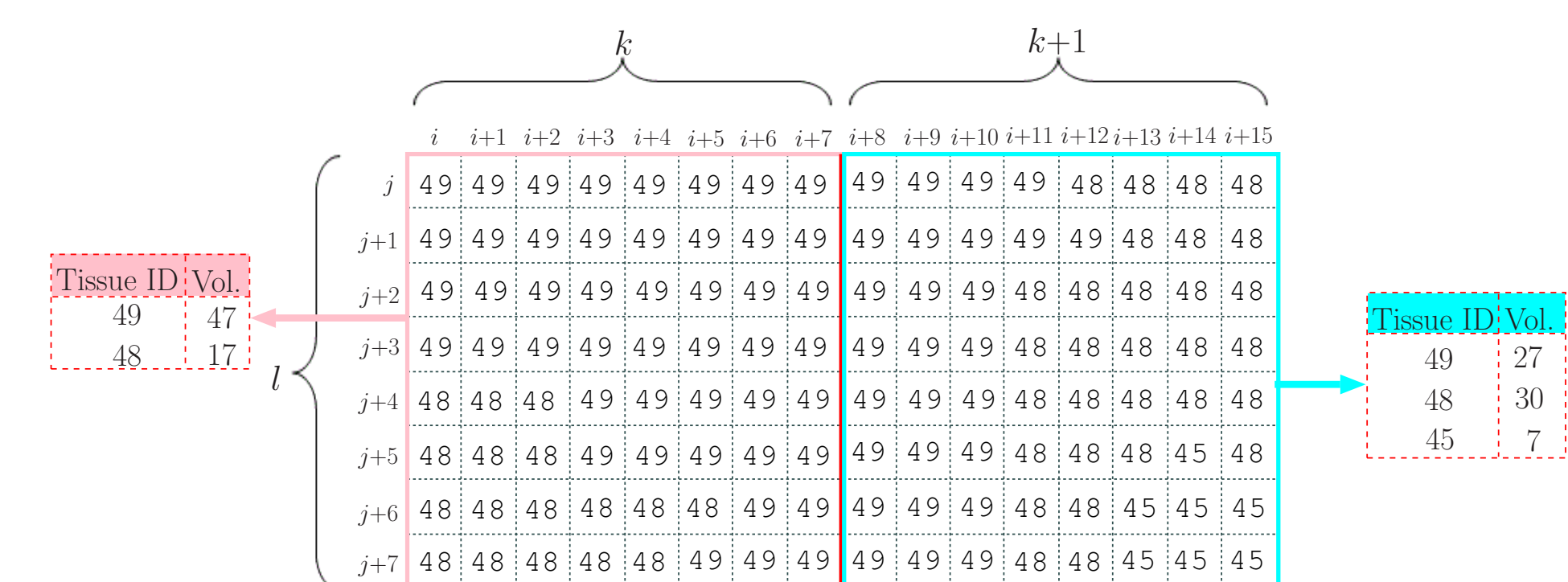


Figure 5: The coarse sampling of the DHP by 8x8, then identification of tissue types and volumes in each coarse cell.

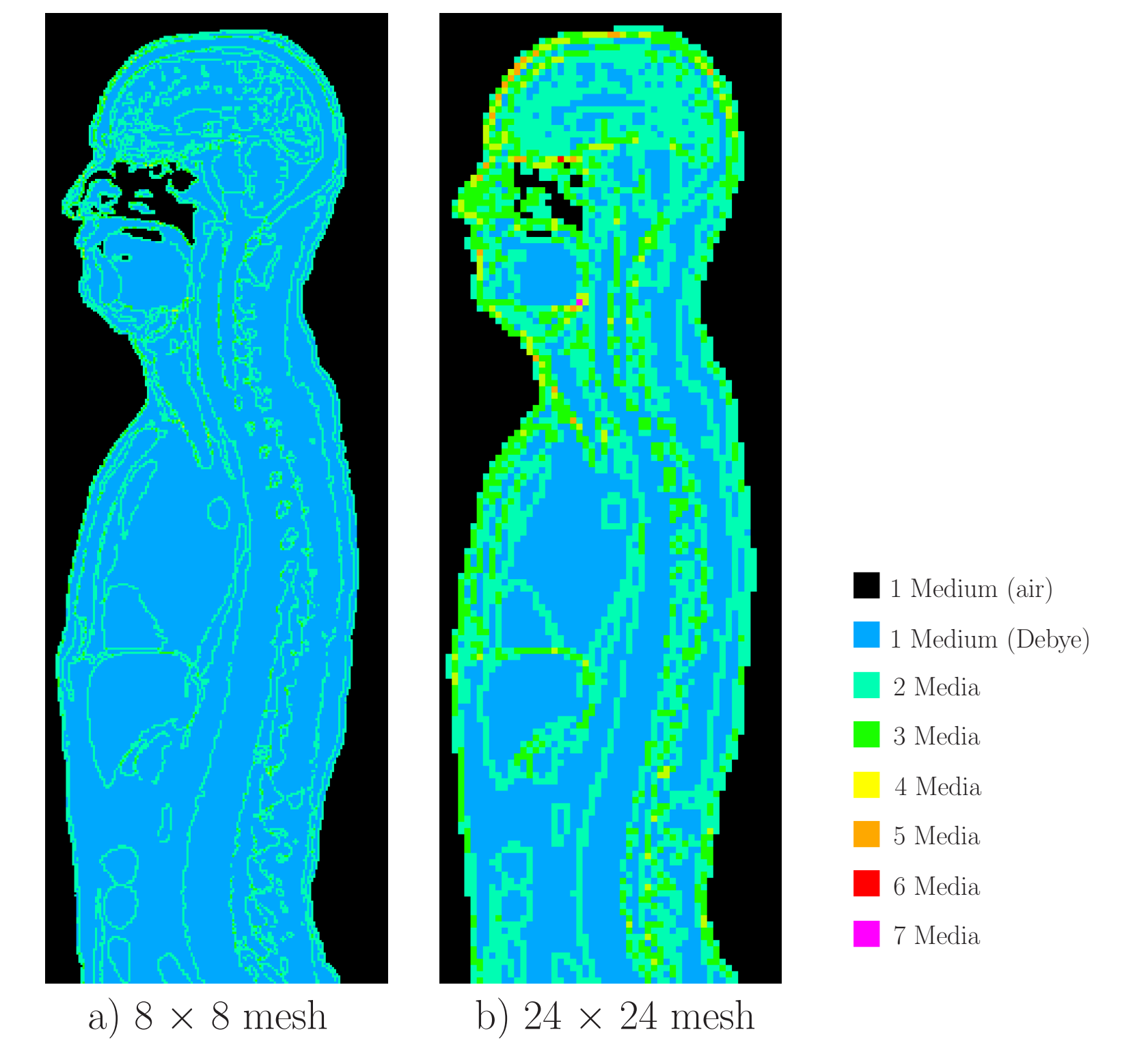


Figure 6: The media mapping of the DHP after coarse meshing

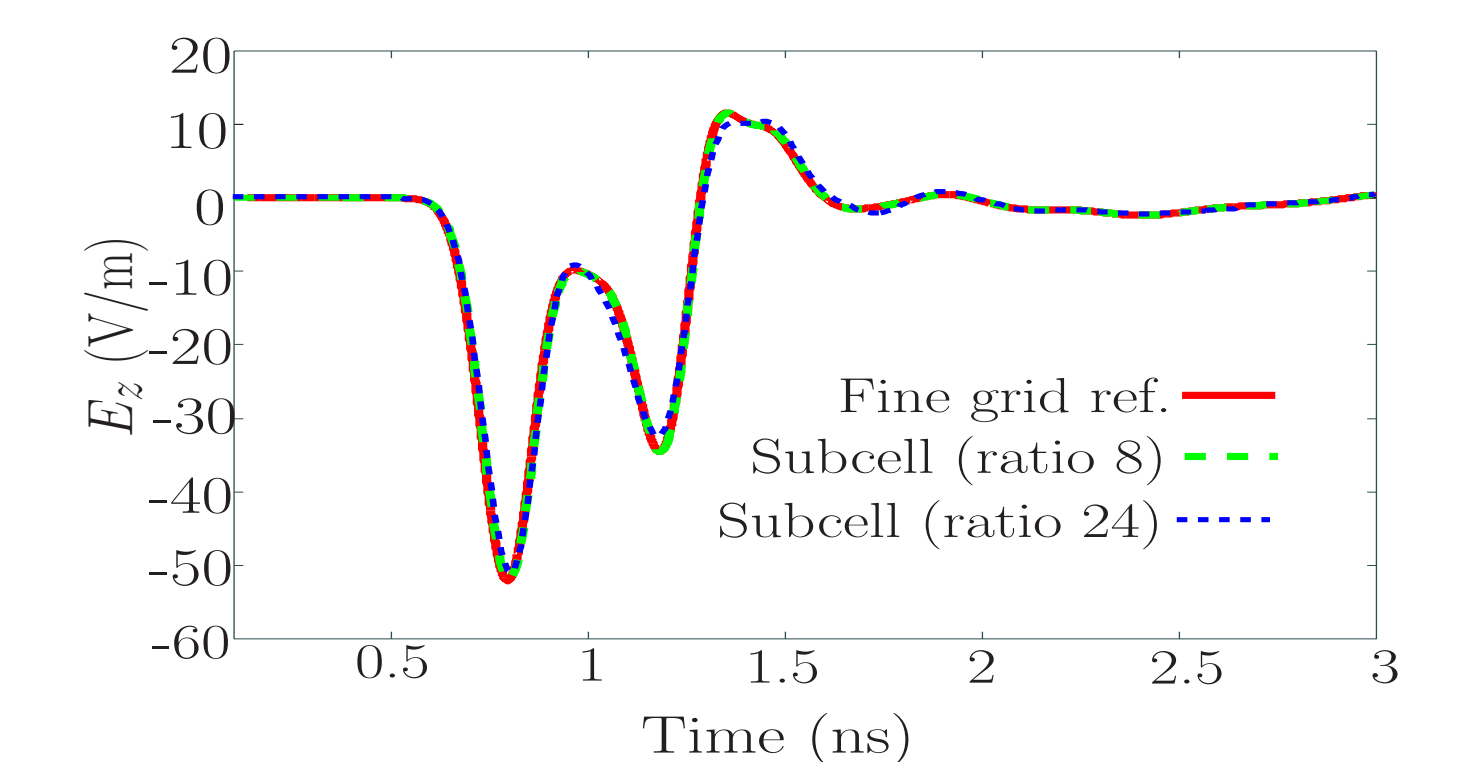


Figure 7: The observation of E_z . The source excitation was a Gaussian pulse and the frequency range was set up to 5.0 GHz.

Subcell Ratio	Total Grid	Memory	Speed up	Relative Error
8	300×600	×14	×37	2.03%
24	100×200	×85	×1342	6.34%

Conclusion

The subcell technique has the potential to be used in numerical applications of bioelectromagnetism, providing dramatic reductions in the computational requirements.

Future Works

- To apply the proposed subcell technique for the simulation of moving, expanding, or contracting frequency-dependent objects.
- To achieve higher computational performance by parallelization of the subcell algorithm in MPI.

Bibliography

- [1] A. Taflov and S.C. Hagness. *Computational Electrodynamics*. Artech House, Norwood, MA, 2005.
- [2] K. Tekbas, F. Costen, J. P. Berenger, R. Himeno, and H. Yokota. Subcell modeling of frequency-dependent thin layers in the FDTD method. *IEEE Transactions on Antennas and Propagation*, 65(1):278–286, Jan 2017.